BJES Basrah Journal for Engineering Sciences

Basrah Journal for Engineering Sciences, Vol. 21, No. 3, (2021), 1-9

Original Article

Journal homepage: www.bjes.edu.iq
ISSN (Online): 23118385, ISSN (Print): 18146120

OPEN ACCESS

An Experimental Study on Micro-Enhanced TESM Incorporated Inside Evacuated Tube Solar Collector Equipped with Heat Pipe

Mohammed J. Alshukri [1,*], Adel A. Eidan [2], Saleh Ismail Najim [3]

[1] *Department of Mechanical Engineering, College of Engineering, University of Kufa, Najaf, Iraq*
[2] *Najaf Technical Institute, Al-Furat Al-Awsat Technical University, Najaf, Iraq*
[3] *Department of Mechanical Engineering, College of Engineering, University of Basrah, Basrah, Iraq*
E-mail addresses: *mohammedj.alshukry@uokufa.edu.iq* , *inj.adel@atu.edu.iq* , *saleh.najim@uobasrah.edu.iq*
Received: 11 May 2021; Accepted: 1 August 2021; Published: 5 October 2021

Abstract

The incorporation of thermal energy storage materials (TESMs) into solar energy systems is a factor that boosts the performance of these systems. In this paper, an experimental study was addressed for enhancing the heat pipe's thermal performance that works with an Evacuated Solar Tube Collector with Heat Pipe (ETCHP) as a solar water heater system. This is done by adding micro-zinc oxide (ZnO-MP) to the paraffin wax integrated as TESM into the evacuated tube (ET) of the system, where the evaporator section of the heat pipe is completely submerged within the micro-enhanced paraffin wax. Three experimental prototype rigs with one evacuated tube were designed, built, and tested to do the investigation. The most important parameters that have been studied in this study are the thermal resistance and the temperature distribution pattern along the heat pipe. The results show a clear indication of the decrease in the thermal resistance of the heat pipe of the proposed system compared to the system in which pure paraffin wax was incorporated. Also, it was noticed that there is a significant improvement in the temperature distribution along the heat pipe due to the improvement in the conductivity of the micro-enhanced wax compared to the pure wax.

Keywords: Evacuated Solar Tube Collector Equipped with Heat Pipe (ESTHP), Paraffin Wax, Micro-Enhanced TESM, GAHP.

http://dx.doi.org/10.33971/bjes.21.3.1

1. Introduction

With the increasing demand for energy used in water heating in both residential and government sectors, there has become an urgent necessity to go to the use of renewable energy as an important source that effectively contributes to reducing dependence on non-renewable sources in heating water in both sectors [1]. On the other hand, the emissions generated by using non-renewable sources are an important incentive to reduce reliance on these sources and move towards the use of renewable energy sources that are environmentally friendly and free from pollution emissions.

Domestic solar water heating systems (DSWHS) are one of the most important applications of solar renewable energy [2]. But it faces challenges and problems that have long occupied the minds of researchers interested in such systems. Providing hot water for long periods, even with diminished solar radiation during the night or overcast sky, is considered one of the most important challenges to ensure attention, which occupied a large number of researches from many researchers in this field. Until now, the use of thermal energy storage materials (TESMs) incorporated into solar systems for heating water is still considered an ideal solution to overcome the problem of the system's inability to supply hot water in the absence of solar radiation. The evacuated tube solar water heater equipped with a heat pipe (ETCHP) is considered one of the most important solar collectors that operate under a high control over the operating hot water temperature, and this is not characteristic of the traditional flat plate collector (FPC). Therefore, the overall efficiency of the ETCHP system greatly exceeds the efficiency of the FPC system.

The ETCHP consists of a copper heat pipe that is partially or completely filled with a working fluid at certain vacuum pressure. The heat pipe consists of two parts, upper and lower, the upper part is called the condenser, while the lower part is known as the evaporator. The heat pipe is centered in the center of two glass cylinders. The space between them is vacuumed to reduce the thermal transfer losses by convection. The outer cylinder is transparent and permeable to solar radiation, while the interior is coated with a dark blue absorbent color to form the absorber of the solar collector. Most of the TESMs incorporated in solar water heating systems are characterized by their low thermal conductivity, and this is a negative indicator that leads to a decrease in the performance of water heating systems.

Many studies have been conducted in order to increase the efficiency of solar water heating systems by incorporating TESM within those systems and thus increasing the possibility of supplying hot water for long times in addition to reducing the temperature difference of the outlet hot water temperature and minimizing the losses of heat. Two investigation studies [3], [4] clarified the importance of integrating TESM into the ETC system. As these studies proved that the incorporation of TESM increased the period of hot water supply and reduced

the temperature fluctuations of the hot water, as well as significantly reduced the amount of heat losses.

Various investigation studies [5]-[11] have been performed on embedded TESM within ETC systems as a thermal booster. Chopra et al. [5] studied the performance of a proposed ETCHP provided with stearic acid as TESM. The new ETCHP operates with a HP and is provided with a water tank charged with TESM. The outcomes noted that, for full-day charging, the system's thermal efficiency varied from around (52-62 %). While, for mid-day charging, the thermal efficiency was varied around (55-72 %). The same authors [6] further performed an investigation of ETCHP provided and not provided TESM for the applying of water heating throughout comparable climate conditions and different water volumetric flow rates. The authors attended the investigation by contrasting the efficiency of a couple of ETCHPs, one collector was included SA-67 inside its ET as a heat storage material, while the other collector was given without TESM as a reference collector. The efficiencies of ETCHP combined with TESM, for 8, 16, 20, and 24 L/h flow rates, were about 37.56 %, 36.69 %, 32.34 %, and 32.73 %, respectively higher than the TESM-free collector. Feliński et al. [7] stated that, according to the solar radiation as well as the TESM's temperature, the yearly efficiency of the collector ranged about 33-66 % with paraffin as TESM. the authors noted that the yearly fraction of the collector with TESM was improved by about (20.5 %) than that of TESM-free. Abokersh et al. [8] investigated an evacuated tube collector with direct flow implemented with TESM (paraffin) has improved efficiency by about 14 % higher than a TESM-free ETC. the authors observed that the overall coefficient of heat losses of the collector combined with TESM ranged by 22.5 % higher than the TESM-free collector. Furthermore, they recorded gain of the energy was about 35.8 and 47.7 % for unequipped and equipped fin ETCs respectively higher than the conventional collector with integrating ($Ba(OH)_2 \cdot 8H_2O$) as TESM. Xue [9] has developed performance, daily useful thermal energy, and mean thermal efficiency for the ETC equipped with (U-shape) HP. Naghavi et al. [10] published that the ETCHP including TESM as a thermal enhancer was further efficient as contrasted with the TESM-free ETC. Papadimitratos et al. [11] investigated the performance of the evacuated tube collector with a couple of different TESMs, i.e., erythritol and tritriacontane. The outcomes showed that the suggested collector's efficiency improved by about 66 and 26 % for stagnation and normal run respectively, contrasted to the traditional model. Féliński and Sekret [12] carried out an investigation study applying TESM (paraffin) included within ETC. The conclusions pointed that the highest and mean charging efficiency of the solar collector improved by 40 to 49 %, and 31 to 36 %, respectively. Li and Zhai [13] assessed the thermal performance of ETCHP with erythritol and extended graphite as composite TESM. The authors recorded that the proposed system, with a solar radiation value of 12.88 MJ/m^2, had 40.17 % mean storage efficiency and heat storage value of 5.17 MJ/m^2. Moreover, investigation research of ETCHP system provided with paraffin as TESM has been performed by Naghavi et al. [14]. On the overcast and sunny days, they detected results ranged (38-32 %) and (34-36 %). The Authors noticed that the flow rate of water directly affects the introduced the efficiency of the collector. Essa et al. [15] mentioned that related to evacuated tube collectors provided with TESM (paraffin), the efficiency of the conventional collector at the lowest flow rate of water was decreased by 21.9 %. The authors also recorded that this enhancement of the collector performance was connected to the complete change phase of the TESM. They observed that the collector's efficiency with TESM integration raised to 6.8 at 1.2 L/min water flow rate. Bazri et al. [16] tested the ETC at different TESMs as a thermal enhancer. The authors concluded that the efficiency of the modified collectors enhanced at an approximate range (36-54 %) compared with TESM-free collector. The efficiency increased by about (46-58 %) on an overcast or rainy day. Boy et al. [17] proposed an improved storage system for ETC equipped with a salt-hydrated TESM for hot water production. The authors noticed that the efficiency improved by using an adequate TESM. Cabeza et al. [18] created a collector system to minimize the water tank's heat losses by placing a TESM system over the tank. Over the water tank, the authors attached many cylinders and investigated the collector's efficiency including 2, 4, and 6 types of TESM. Mettawee and Assassa [19] examined the performance of the individual TESM flat-panel collector. in the proposed study, The TESM system has directly worked as an absorber for solar radiation. Tarhan et al. [20] conducted an investigation study with three various trapezoidal solar collectors to examine the influence of TESM applications, the location of the absorptive plate and TESM, on the collector's efficiency. Moreover, the sensible and latent TESS and the thermo-packed bed part for the solar collector used to produce hot water were studied by Nallusamy et al. [21]. El Qarnia [22] analyzed the theoretical study of a solar TES system including within a set of comparable tubes embedded inside the TESM. The authors observed that the collector transferred a heated fluid inside the tubes and divided the incident solar energy inside the TESM tank. According to the literature, the TESM-based storage systems have been separated from solar collectors or directly put inside the collectors on the flat panel.

This article studied the thermal performance of a modern ECTHP with including TESM inside its ET as demonstrated in Fig. 1. Therefore, the influence of the TESM on the rate of heat transfer was examined by employing paraffin wax as TESM placed inside ET of the ETCHP. Additionally, the limitation of enhancing the pure thermal conductivity of the selected TESM by using ZnO as a high thermal conductivity micro-material was studied in this research. Due to supplying a delayed heat to an ETCHP in case of low or unavailable solar radiation at nighttime or when the sky is overcasting, the incorporation of TESM in the (ET) represents an important role in solar collectors used for water heating. To the authors' knowledge, the thermal performance investigation of ETCHP with TESM enhanced with micro-particles incorporated within ET has not been researched until now.

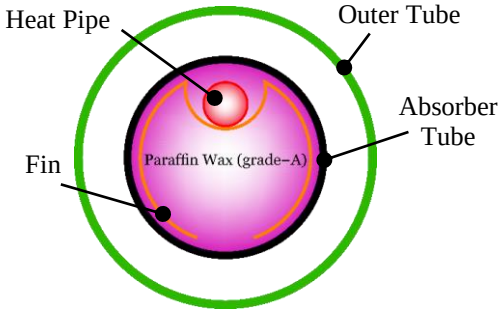

Fig. 1 Location of integrated TESM within HP.

2. Selection of Materials

2.1. Selection of TESM

TESM choice for each utilization is according to a set of parameters, for example, high thermal conductivity, adequate temperature limit, high thermal/chemical stability, and proper latent heat. The selection of TESM, based upon those distinct parameters, is an essential decision. Furthermore, it is reasonable to distribute TESMs to a couple of types with high and low melting temperatures.

Paraffin (C_nH_{2n+2}) is a chemical material valuable with moderate and low melting points, non-toxic and non-flammable, physically stable, low-priced, and widely available. Those features raised the stimulus to apply paraffins as TESM in solar water heater collectors. Based upon the carbon atoms number (n), there are wide melting point ranges (6-85 °C) and heat of fusion (225-275 kJ/kg) for paraffins. So, the suitable paraffin is chosen for TES application according to the working temperature and the melting and solidifying temperature range.

Because of a high melting point TESMs, require a lengthy time to completely melt, and a considerable amount remains in solid-state. Consequently, TESMs with a high melting point are not an ideal choice for medium or low-temperature collectors. Many types of paraffin wax are not suitable for incorporation into the evacuated tube of the solar collector due to the high temperatures that the inner surface of the evacuated tube reaches due to the vacuum layer and the accumulation of solar energy during the collector operation to the layer. Therefore, the selection of suitable TESM with a proper melting point within the ET for solar energy storage is relatively difficult. The grade (A) paraffin wax from the Al-Dora oil refinery in Baghdad-Iraq was chosen within the ET as TESM with a medium melting point. Table 1 shows the properties of the chosen TESM in this research.

Table 1. The chosen TESM's thermophysical properties.

Properties	Paraffin (Grade-A)	Unit
Melting temperature	64	°C
Latent fusion heat	268	kJ/kg
Solid state density	787.9	kg/m^3
Liquid state density	765.4	kg/m^3
Thermal conductivity	0.211	W/m °C
Solid state Cp	2.775	kJ/kg °C
Liquid state Cp	2.29	kJ/kg °C

2.2. Selection of Micro-Material

It is important to select the relevant material from the convenient micro and nanomaterials added to the TESM to achieve an enhanced thermal efficiency of solar collectors. It is evident that the nano and microcomputer additives significantly change the physical properties of the materials used, which are the main parameter of the solar collector's performance which integrated with TESMs. This requires studying the physical properties of the compounds of TESMs and these additives, which in turn enables us to choose the optimal materials.

The availability and health hazards are the principal limitations to utilizing nanomaterials. For these reasons, in this experimental study, it is suggested to use micromaterials instead of nanomaterials. So, an additive of ZnO micromaterial with 5 % wt was chosen as a thermal conductivity booster for selected paraffin wax. The micro-ZnO thermophysical properties were presented in Table 2 [23].

Table 2. Thermophysical properties of ZnO-MP.

Properties	Specifications	Unit
Appearance	White	---
Density	5607	kg/m^3
Thermal conductivity	1.21	W/m K
Specific heat constant	495	J/kg K
D_p	55	µm

3. Experimental Rig and Procedure

The experiment was carried out in an outdoor environment for this research. It was tested at Najaf, Iraq (Latitude 32° 1' 33.4" N, and Longitude 44° 20' 46.5" E). The data were collected in January 2020. The ETCHP's specification details are present in Table 3 [23].

Table 3. The specification details of ETCHP.

Solar Collector	
Properties	**Specifications**
Type	Heat pipe–evacuated tube collector
Collector area	0.0692 m^2
Gravitational Assist Heat Pipe (GAHP)	
Properties	**Specifications**
Inner diameter	1.4 cm
Outer diameter	1.6 cm
Condenser length	20 cm
Evaporator length	115 cm
Working fluid	Acetone
Material	Copper
Glass Envelope	
Properties	**Specifications**
Inner diameter	4.5 cm
Outer diameter	5 cm
Wall thickness	0.25 cm
Length	120 cm
Vacuum	10 - 4 torr
Material	Glass (Pyrex)
Flat Reflector	
Properties	**Specifications**
Area	1.3 × 0.35 m
Material	Aluminum sheet foil
Hot Water Tank	
Properties	**Specifications**
Capacity	5 L
Insulation	5 mm Fiber Glass + 0.3 cm Silicon + Layer of Glass Wool
Outer shell	Sheet of 0.3 cm Alicabond
Material	Aluminum with thickness 0.1 cm

Three identical ETCHP with single ET were employed to examine the impact of combining TESM inside the ET on the thermal performance of these collectors, as shown in Fig. 2. Every collector was placed southward with a 45° horizontal inclination angle. The ETCHP-B includes ET charged with 0.9 kg of (grade-A) paraffin wax surrounded the HP. Also, the ETCHP-C was identical to the ETCHP-B except for the difference in the incorporated paraffin wax which was enhanced with ZnO microparticles. The ETCHP-A has assumed a reference collector where it was left TESM-free. The three investigated collectors' details were illustrated in Table 4 referring to the TESM integration location.

Table 4. The three used collectors' details.

Collector's Code	Location of TESM	Types of TESM
ETCHP-A	Without TESM	---
ETCHP-B	ET	Paraffin (grade-A)
ETCHP-C	ET	Paraffin (grade-A) + ZnO-MP

The HP in the tested collectors was charged with a charging ratio of 70 % of pure acetone. Throughout the test, twenty-three temperature sensors K-type were employed to evaluate the temperature within the HP and the manifold. The thermocouples inside the HP were placed in different positions and levels to establish an accurate and stable measure of the energy inside it. As displayed in Fig. 3, five thermocouples were situated in the center of every cross-section at various positions to correctly estimate the evaporator and condenser's temperature (2 and 3 in the condenser and evaporator section respectively).

The evaporator and condenser's temperature sensors' recording allows the condensation and boiling processes within the HP to be clearly studied. Moreover, the mean water temperature within the manifold was measured by reading another 5 thermocouples arranged in many positions of the manifold [23].

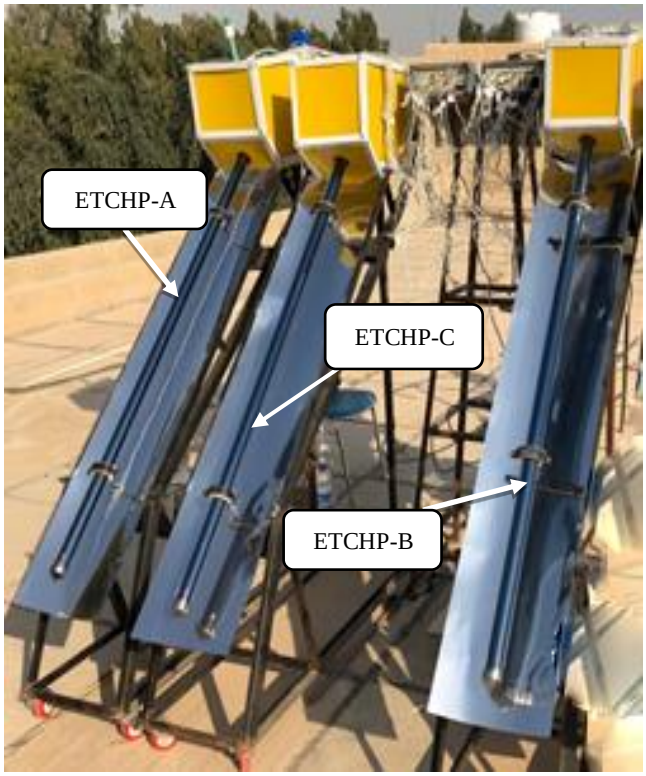

Fig. 2 A Schematic of the three studied ETCHPs.

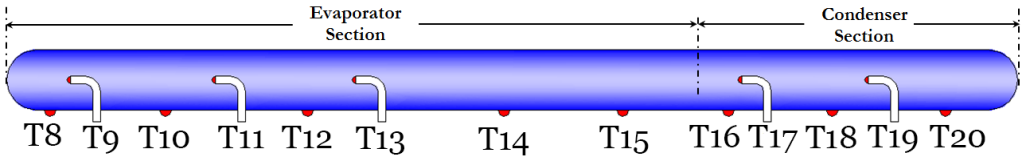

Thermocouple No.	T_8	T_9	T_{10}	T_{11}	T_{12}	T_{13}	T_{14}	T_{15}	T_{16}	T_{17}	T_{18}	T_{19}	T_{20}
Position (mm)	10	30	250	500	565	750	1000	1100	1160	1230	1230	1280	1280

Fig. 3 Locations of HP's thermocouples.

The performance parameters are examined for a couple of water flow rate values (i.e. 1 and 2 L/h). As demonstrated in Fig. 4, each ETCHP was provided with water from a separate tank with a volume of 20 L. The upper cover of each tank is removed to leave open with the atmosphere for dispersing thermal energy, acting as the hot water delivered. The water is provided from the base of the manifold to minimize the influence of returning the hot water to the manifold again. The manifold's temperature, the atmospheric temperature, inlet and outlet temperatures of the manifold, and the wall and center temperatures of all HP were estimated over the test time.

For the HP's thermal performance evaluations, the overall thermal resistance of the HP can be estimated by:

$$(R_{hp})_{without\ (TESM)} = \frac{\bar{T}_{eva} - \bar{T}_{cond}}{\pi \times D_{abs} \times l_{eva} \times I} \quad (1)$$

$$(R_{hp})_{with\ (TESM)} = \frac{\bar{T}_{eva} - \bar{T}_{cond}}{\pi \times D_{abs} \times l_{eva} \times I + \frac{m_{TESM} \times L_{TESM}}{3600} + \frac{m_{TESM} \times C_{p(TESM)} \times \Delta T_{TESM}}{3600}} \quad (2)$$

Where $\bar{T}_{cond}$ and $\bar{T}_{eva}$ is the condenser and evaporator mean wall temperature respectively, measured by 8 thermocouples located at various positions on the external surface of the heat pipe as illustrated in Fig. 4, L_{eva} is the length of the evaporator in (m), and Dabs is the diameter of the absorber in (m).

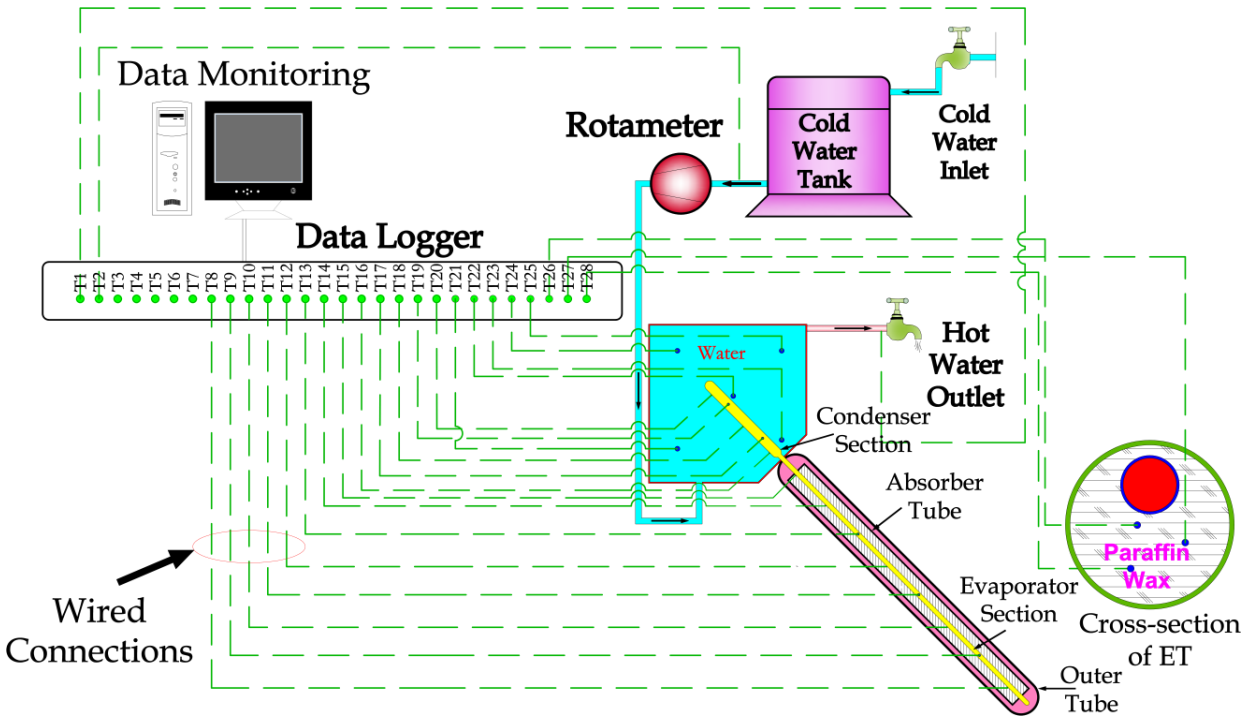

Fig. 4 Experimental ETCHP rig's schematic diagram.

4. Uncertainty

Principally, an important measure is inadequate to be determined explicitly according to several parameters which are immediately assessed, i.e. R = *f* (T_1, T_2, T_3, T_4 …). The determined parameters (X_1, X_2, X_3, X_4 …) a roughly various quantity which is named uncertainty. The analysis tries to estimate the uncertainties in every one of the measured variables into the calculated measure values. The flowing equation is used to evaluate the uncertainties:

$$U_R = \sqrt{\sum_i \left(\frac{\partial R}{\partial T_i}\right)^2 U_{T_i}^{\ 2}} \quad (3)$$

Where U_R means the uncertainty of the variable.

In general, the determining parameters are according to the identified values. Table 5 lists the uncertainties of the devices used in the experimental investigation [23].

Table 5. Instruments' uncertainties.

Measured parameters	Instrument's details	Mean value	Total uncertainty value	Total uncertainty (%)
Temperature measurement, °C	Thermocouple type-K	45	± 0.41	± 0.91
Volumetric flow rate meter, L/h	Lzb-S water rotameter	1	± 0.4	± 1.4
Solar meter, W/m^2	TM-207 solar power meter	400	± 0.5	± 1.6

5. Results and Discussion

In this section, the performance parameters such as temperature distribution along the evaporator section and thermal resistance of the heat pipe have been discussed for different water flow rates (i.e. 1 and 2 L/h).

5.1. Evaporator Section Temperature Distribution

Fig. 5 (a) and (b) demonstrates the influence of incorporation of pure and enhanced ZnO-MP paraffin wax within the ET of ETCHP-B and ETCHP-C respectively, on wall temperature of the evaporator as contrasted with ETCHP-A at a water flow rate of 1 L/h. From Fig. 5 (a) it was shown that the evaporator wall temperature of ETCHP-B at 8:00 AM remains less than that of ETCHP-A. This is because of the time it needs for the TESM to melt. Hence, the heat transfer rate through TESM to the evaporator wall will decrease. Though, for ETCHP-B, it was noted that there was a rise in the temperature throughout the evaporator length at 10:00 AM and 12:00 PM. The cause for this rise is the pure paraffin wax's latent heat through the process of phase change. For ETCHP-B at 8:00 AM, there was a small variation in readings recorded from the four thermocouples named T_8, T_{10}, T_{12}, and T_{14} which were placed on the outer surface of the evaporator. In the meanwhile, the reading of T_{15} thermocouple recorded a significant reduction because of its position near the condenser. With time, the reading recorded from all the five thermocouples becomes uniform because of the entirely melting of paraffin. Accordingly, the heat transfer between the TESM and the outer surface of the evaporator will be uniform. Wherever it was recorded that the highest difference between the readings of T_8, T_{10}, T_{12}, T_{14}, and T_{15} at 8:00 AM, 10:00 AM, and 12:00 PM was 10, 7.3, and 3 °C respectively. On the other hand, from Fig. 5 (b) it can be noticed a relatively high jump in the evaporator surface temperature. The reason for this is due to the significant improvement in the thermal

conductivity of paraffin wax due to the addition of ZnO-MP. Therefore, the rate of heat transfer through the wax will increase significantly due to this increase in the conductivity of the wax. Also, increasing the rate of heat transfer greatly accelerates the melting of paraffin wax, so the heat transfer mechanism shifts from conduction heat transfer through solid wax to convective heat transfer through liquid wax. This is clearly evident by the higher temperature of the evaporator surface surrounded by the ZnO-MP-enhanced paraffin wax than it is in the evaporator surrounded by the pure paraffin wax. Also, adding the ZnO-MP additives to the wax led to a uniform temperature distribution along the evaporator compared with the reference collector. Where the achieved maximum difference between the five outer thermocouples' temperatures were about 8.5, 13.44, and 11.1 °C for 8:00 AM, 10:00 AM, and 12:00 PM respectively.

Fig. 6 (a) and (b) show that increasing the flow rate from 1 to 2 L/h causes a slight decrease in the temperature of the outer surface of the evaporator surrounded by pure or enhanced paraffin wax, especially the temperature read by the sensors far from the condenser.

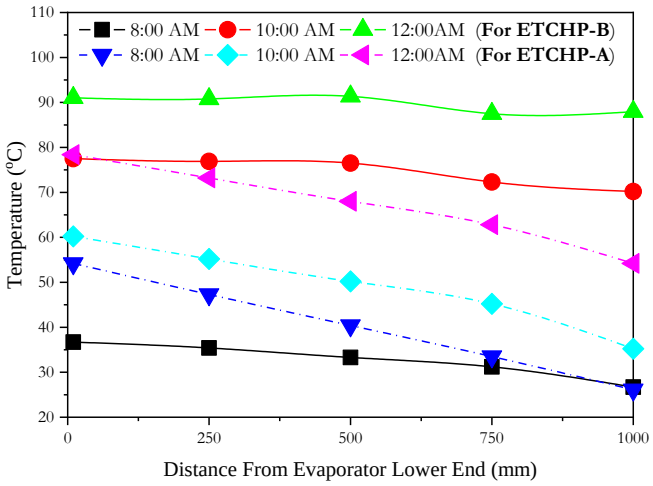

(a)

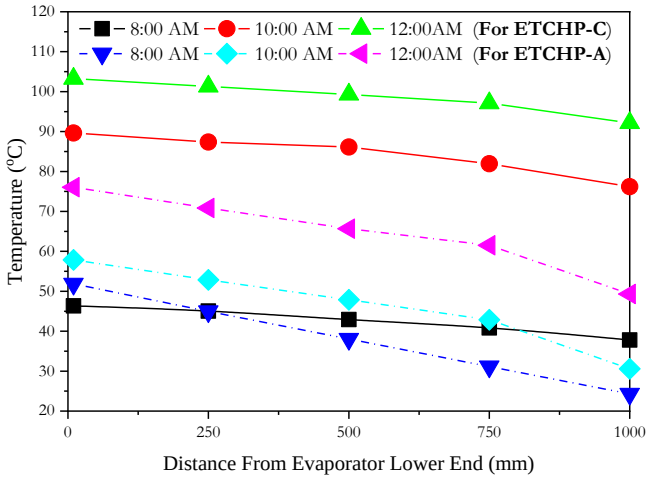

(b)

Fig. 5 The wall temperature distribution along evaporator section at 1 L/h (a) between ETCHP-B and A. (b) between ETCHP-C and A.

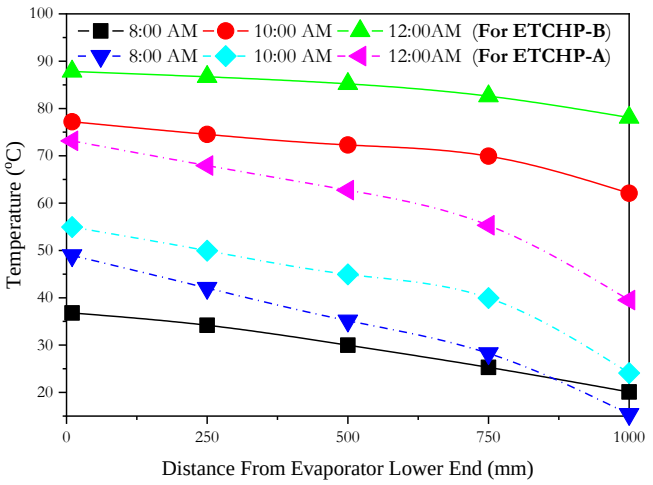

(a)

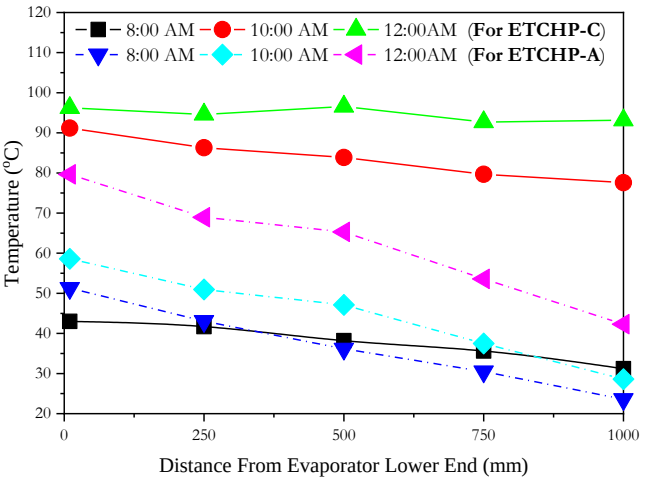

(b)

Fig. 6 The wall temperature distribution along evaporator section at 2 L/h (a) between ETCHP-B and A. (b) between ETCHP-C and A.

The reason for not being affected by the increased flow rate is the thermal storage of the wax, which compensates for the heat losses resulting from the amount of heat lost through the condenser to the coolant water. While it is noticed that the evaporator temperature of the reference solar collector is clearly affected by an increase in the rate of water flow, as there is no thermal storage that compensates for the decrease in heat resulting from the heat exchange processes at the condenser surface. So, it was observed that the highest differences between the five outer sensors' temperatures were about 27.7, 30, and 37.34 °C for 8:00 AM, 10:00 AM, and 12:00 PM respectively for ETCHP-A. While the highest differences between the five outer thermocouples' temperatures were about 16.7, 15.1, and 9.72 °C for 8:00 AM, 10:00 AM, and 12:00 PM respectively for ETCHP-B. Also, it was seen that the highest temperature difference between the five outer sensors was about 11.8, 13.6, and 3 °C for 8:00 AM, 10:00 AM, and 12:00 PM respectively for ETCHP-C.

5.2. Variation of HP's thermal resistance

The difference of HP's thermal resistance throughout the charging time is presents in Fig. 7 (a) and (b) for a flow rate of 1 and 2 L/h respectively. It was noted that the incorporation of pure or enhanced TESM within the (ET) significantly

decreases the total heat pipe's thermal resistance compared with the reference collector (ETCHP-A). That is due to the uniformed heat absorbed by the surface of the evaporator section. Therefore, the heat transfers along the heat pipe's surface to the liquid acetone approximately by convection heat transfer mechanism at a uniform wall temperature. This is demonstrated by the close readings of the five sensors installed at different locations on the evaporator outer wall of ETCHP-B and ETCHP-C. Therefore, it was obvious that ZnO-MP-enhanced paraffin wax has a more remarkable influence on thermal resistance than pure paraffin wax. From Fig. 7 (a), it was shown that at 1 L/h the thermal resistance value was (0.23-0.95 °C/W), (0.244-1.19 °C/W), and (0.353-1.29 °C/W) for ETCHP-C, ETCHP-B, and ETCHP-A respectively. With an increase in the rate of water flow to 2 L/h, the heat transmitted between the outer surface of the condenser and the water moving around it increases and so the temperature of the condenser surface reduces.

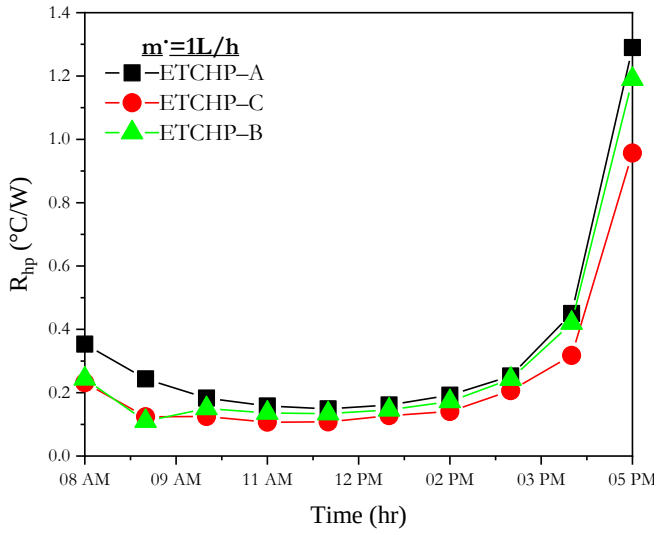

Fig. 7 Thermal resistance fluctuation for the HP throughout the charging time for (a) ṁ = 1 L/h (b) ṁ = 2 L/h.

Moreover, the evaporator temperature is slightly affected by increasing the water flow rate because of the accumulated heat in the TESM embedded in the ET. Therefore, the change in the thermal resistance of the heat pipe changes proportionally with the change in the water flow. As a result of increasing the temperature difference between evaporator and condenser outer walls temperatures. There is an increase in R_{hp} with increasing of water flow rate to 2 L/h. Hence, from Fig. 7 (b), it was seen that the thermal resistance value for ETCHP-C, ETCHP-B, and HPETC-A were (0.32-1.06 °C/W), (0.314-1.25 °C/W), and (0.25-1.69 °C/W) respectively at the water flow rate of 2 L/h.

6. Conclusions

The current research studies an experimental investigation of boosting the thermal performance of the (ETCHP) by incorporating micro ZnO-enhanced paraffin wax as a thermal energy storage material (TESM) within the collector's ET. Therefore, two tests were done to examine the incorporation of enhanced paraffin wax into only the (ET) with a couple of water flow rates (i.e. 1 and 2 L/h). The following conclusions are summarized:

1. Incorporating TESM into the evacuated tube helps to overcome the problem of overheating that is not desirable for the heat pipe, especially in areas with high levels of solar radiation compared to the reference collector.
2. Incorporating pure paraffin wax into the evacuated tube significantly improves the thermal performance of the heat pipe by making the heat exchange mechanism between the evaporator surface and the working fluid take place very close to the convection heat transfer at a constant surface temperature.
3. Due to the improvement in the thermal conductivity of the enhanced wax caused by the ZnO-MP additives, the thermal performance of the heat pipe surrounded by the ZnO-MP-enhanced paraffin wax is better than the thermal performance in the case of it surrounded by the pure paraffin wax.
4. The temperature fluctuations are reduced along the evaporator surface surrounded by the ZnO-MP enhanced wax and the surface temperatures are higher than in the case of pure paraffin wax.
5. The thermal resistance of the heat pipe surrounded by the ZnO-MP enhanced paraffin wax decreases greater than that of the heat pipe surrounded by the pure paraffin wax.

References

[1] M. A. Fazilati, A. A. Alemrajabi, "Phase change material for enhancing solar water heater, an experimental approach", Energy Conversation and Management, Vol. 71, pp.138-145, 2013. https://doi.org/10.1016/j.enconman.2013.03.034

[2] M. J. Muhammad, I. A. Muhammad, N. A. Che Sidik, M. N. A. W. Muhammad Yazid, "Thermal performance enhancement of flat-plate and evacuated tube solar collectors using nanofluid: A review", International Communications in Heat and Mass Transfer, Vol. 76, pp. 6-15, 2016. https://doi.org/10.1016/j.icheatmasstransfer.2016.05.009

[3] R. Daghigh, A. Shafieian, "Theoretical and experimental analysis of thermal performance of a solar water heating system with evacuated tube heat pipe collector", Applied Thermal Engineering, Vol. 103, pp. 1219-1227, 2016. https://doi.org/10.1016/j.applthermaleng.2016.05.034

[4] W. Lin, Q. Wang, X. Fang, X. Gao, Z. Zhang, "Experimental and numerical investigation on the novel latent heat exchanger with paraffin/expanded graphite

composite", Applied Thermal Engineering, Vol. 144, pp. 836-844, 2018. https://doi.org/10.1016/j.applthermaleng.2018.08.103

[5] K. Chopra, V. V. Tyagi, A. K. Pathak, A. K. Pandey, and A. Sari, "Experimental performance evaluation of a novel designed phase change material integrated manifold heat pipe evacuated tube solar collector system", Energy Conversation and Management, Vol. 198, 2019. https://doi.org/10.1016/j.enconman.2019.111896

[6] K. Chopra, A. K. Pathak, V. V. Tyagi, A. K. Pandey, S. Anand, and A. Sari, "Thermal performance of phase change material integrated heat pipe evacuated tube solar collector system: An experimental assessment", Energy Conversation and Management, Vol. 203, 2020. https://doi.org/10.1016/j.enconman.2019.112205

[7] P. Feliński and R. Sekret, "Effect of PCM application inside an evacuated tube collector on the thermal performance of a domestic hot water system", Energy and Buildings, Vol. 152, pp. 558-567, 2017. https://doi.org/10.1016/j.enbuild.2017.07.065

[8] M. H. Abokersh, M. El-Morsi, O. Sharaf, and W. Abdelrahman, "On-demand operation of a compact solar water heater based on U-pipe evacuated tube solar collector combined with phase change material", Solar Energy, Vol. 155, pp. 1130-1147, 2017. https://doi.org/10.1016/j.solener.2017.07.008

[9] H. S. Xue, "Experimental investigation of a domestic solar water heater with solar collector coupled phase-change energy storage", Renewable Energy, Vol. 86, pp. 257-261, 2016. https://doi.org/10.1016/j.renene.2015.08.017

[10] M. S. Naghavi, K. S. Ong, I. A. Badruddin, M. Mehrali, M. Silakhori, and H. S. C. Metselaar, "Theoretical model of an evacuated tube heat pipe solar collector integrated with phase change material", Energy, Vol. 91, pp. 911-924, 2015. https://doi.org/10.1016/j.energy.2015.08.100

[11] A. Papadimitratos, S. Sobhansarbandi, V. Pozdin, A. Zakhidov, and F. Hassanipour, "Evacuated tube solar collectors integrated with phase change materials", Solar Energy, Vol. 129, pp. 10-19, 2016. https://doi.org/10.1016/j.solener.2015.12.040

[12] P. Feliński and R. Sekret, "Effect of a low cost parabolic reflector on the charging efficiency of an evacuated tube collector/storage system with a PCM", Solar Energy, Vol. 144, pp. 758-766, 2017. https://doi.org/10.1016/j.solener.2017.01.073

[13] B. Li and X. Zhai, "Experimental investigation and theoretical analysis on a mid-temperature solar collector/storage system with composite PCM", Applied Thermal Engineering, Vol. 124, pp. 34-43, 2017. https://doi.org/10.1016/j.applthermaleng.2017.06.002

[14] M. S. Naghavi, K. S. Ong, I. A. Badruddin, M. Mehrali, and H. S. C. Metselaar, "Thermal performance of a compact design heat pipe solar collector with latent heat storage in charging/discharging modes", Energy, Vol. 127, pp. 101-115, 2017. https://doi.org/10.1016/j.energy.2017.03.097

[15] M. A. Essa, N. H. Mostafa, and M. M. Ibrahim, "An experimental investigation of the phase change process effects on the system performance for the evacuated tube solar collectors integrated with PCMs", Energy Conversation Management, Vol. 177, pp. 1-10, 2018. https://doi.org/10.1016/j.enconman.2018.09.045

[16] S. Bazri, I. A. Badruddin, M. S. Naghavi, O. K. Seng, and S. Wongwises, "An analytical and comparative study of the charging and discharging processes in a latent heat thermal storage tank for solar water heater system", Solar Energy, Vol. 185, pp. 424-438, 2019. https://doi.org/10.1016/j.solener.2019.04.046

[17] E. Boy, R. Boss, and M. Lutz, "A collector storage module-with integrated phase change material", Proc. ISES Pergamon Press Hambg., pp. 3672-3680, 1987. https://doi.org/10.1115/POWER-ICOPE2017-3520

[18] L. F. Cabeza, M. Ibáñez, C. Solé, J. Roca, and M. Nogués, "Experimentation with a water tank including a PCM module", Solar Energy Materials and Solar Cells, Vol. 90, Issue 9, pp. 1273-1282, 2006. https://doi.org/10.1016/j.solmat.2005.08.002

[19] E. B. S. Mettawee and G. M. R. Assassa, "Experimental study of a compact PCM solar collector", Energy, Vol. 31, Issue 14, pp. 2958-2968, 2006. https://doi.org/10.1016/j.energy.2005.11.019

[20] S. Tarhan, A. Sari, and M. H. Yardim, "Temperature distributions in trapezoidal built in storage solar water heaters with/without phase change materials", Energy Conversion and Management, Vol. 47, Issues 15-16, pp. 2143-2154, 2006. https://doi.org/10.1016/j.enconman.2005.12.002

[21] N. Nallusamy, S. Sampath, and R. Velraj, "Experimental investigation on a combined sensible and latent heat storage system integrated with constant/varying (solar) heat sources", Renewable Energy, Vol. 32, Issue 7, pp. 1206-1227, 2007. https://doi.org/10.1016/j.renene.2006.04.015

[22] H. El Qarnia, "Numerical analysis of a coupled solar collector latent heat storage unit using various phase change materials for heating the water", Energy Conversation and Management, Vol. 50, Issue 2, pp. 247-254, 2009. https://doi.org/10.1016/j.enconman.2008.09.038

[23] M. J. Alshukri, A. A. Eidan, and S. I. Najim, "Thermal performance of heat pipe evacuated tube solar collector integrated with different types of phase change materials at various location", Renewable Energy, Vol. 171, pp. 635-646, 2021. https://doi.org/10.1016/j.renene.2021.02.143

Biographies

Mohammed J. Alshukri received the B.Sc. degree in Mechanical Engineering from Dept. of Mechanical Engineering, Faculty of Engineering, University of Kufa, Najaf, Iraq in 2006. He received the M.Sc. degree in "Thermal Power" from University of Technology, Baghdad, Iraq in 2012. He is also still a Ph.D. student in Dept. of Mechanical Engineering, College of Engineering, University of Basrah, Basrah, Iraq. He worked as a teaching assistant and an instructor in the Dept. of Mechanical Engineering, Faculty of Engineering, University of Kufa, Najaf, Iraq from 2012 until now.

Adel A. Eidan received the B.Sc. degree in Mechanical Engineering from Dept. of Mechanical Engineering / Air Conditioning and Refrigeration, University of Technology, Baghdad, Iraq in 2000. He received the M.Sc. degree in "Air Conditioning and Refrigeration" from University of Technology, Baghdad, Iraq in 2003. He also received the Ph.D. degree in "Thermal Mechanics" from Dept. of Mechanical Engineering, College of Engineering, University of Basrah, Basrah, Iraq in 2016. He worked as a teaching staff in the Dept. of Air Conditioning and Refrigeration, Technical Institute of Najaf, Al-Furat Al-Awsat Technical University, Najaf, Iraq from 2003 to 2019 then as an Assistant Professor from 2019 until now. He had assumed the position of Dean Assistant of Technical Institute of Najaf.

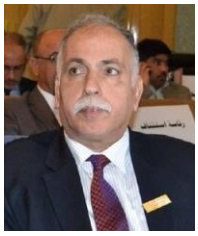

Saleh Ismail Najim received the B.Sc. degree in Mechanical Engineering from Dept. of Mechanical Engineering, College of Engineering, University of Basrah, Basrah, Iraq in 1972. He received the Ph.D. degree in "combustion and energy" from University of Wales, Cardiff, U.K. in 1979. He worked as a teaching staff in the Dept. of Mechanical Engineering, College of Engineering, University of Basrah, Basrah, then as a Professor from 1998 until now. He had held several times the post of Head of the Dept. of Mechanical Engineering, Dean Assistant, and Dean at the College of Engineering, University of Basrah. Also, he had assumed the position of President of University of Basrah.